Hindawi
International Journal of Antennas and Propagation
Volume 2017, Article ID 3595620, 7 pages
https://doi.org/10.1155/2017/3595620

Research Article

Wideband Circularly Polarized Spidron Fractal Slot Antenna with an Embedded Patch

Amir Altaf,[1] Youngoo Yang,[2] Kang-Yoon Lee,[2] and Keum Cheol Hwang[2]

[1]*Division of Electronics and Electrical Engineering, Dongguk University, Seoul 04620, Republic of Korea*
[2]*School of Electronic and Electrical Engineering, Sungkyunkwan University, Suwon 16419, Republic of Korea*

Correspondence should be addressed to Keum Cheol Hwang; khwang@skku.edu

Received 5 March 2017; Accepted 10 April 2017; Published 27 April 2017

Academic Editor: N. Nasimuddin

In this communication, a wideband circularly polarized (CP) Spidron fractal microstrip antenna is proposed based on the concept of embedded structures. The proposed antenna is excited by a tapered microstrip feedline. A wide 3 dB axial ratio (AR) bandwidth of 28.81% (3.09–4.13 GHz) is obtained by merging the CP bands of the Spidron fractal slot and patch antennas. In addition, a measured −10 dB reflection bandwidth of 47.25% (2.57–4.16 GHz) is reported. The measured results are in reasonable concurrence with the simulated results. The measured gain varies between 2.12 dBic and 3.56 dBic within the AR bandwidth.

1. Introduction

In modern communication systems, microstrip fractal antennas (MFAs) are useful due to their low profile, light weight, multiband or broadband capabilities, and ease of fabrication. Mostly, MFAs have been utilized as linearly polarized (LP) antennas, with the design objectives of broadband or multiband characteristics and size reductions [1–3].

Circularly polarized (CP) MFAs are usually preferred over the LP type because they offer advantages such as flexible orientation between the transmitter and receiver, the mitigation of multipath interference, and good mobility. In the literature, a single-feed method is employed for the excitation of circular polarization in MFAs, which require less space but possess a narrow 3 dB axial ratio (AR) bandwidth [4, 5]. To cope with the demand for modern wireless communication, a microstrip-fed fractal slot design with a 3 dB AR bandwidth of 22% has been developed [6]. However, only simulated results were presented. Recently, symmetric slot antennas have been proposed and designed in an effort to enhance the AR bandwidth [7, 8].

This study presents a simple and effective technique based on the notion of an embedded structure for the design of a compact wideband CP MFA. The proposed design consists of a Spidron fractal slot with an added rectangular slit and an embedded Spidron fractal patch. A microstrip tapered feedline is deployed for excitation, alleviating the use of a hybrid coupler [9]. Wide reflection and an AR bandwidth are obtained by merging the resonance and CP bands of the Spidron fractal slot and the patch. Details of the proposed antenna design along with the experimental results are discussed in the following sections.

2. Antenna Design

Figure 1 shows the geometry of the proposed Spidron fractal planar antenna, which is fabricated on a square Taconic RF-35 substrate with a dielectric constant (ε_r) of 3.5, with the width denoted by g_w and thickness h. The construction of a Spidron fractal system for a slot antenna was initially proposed in earlier work [10]. A seven-iterated Spidron fractal slot with adjacent side length h_1 and angle α is etched from the ground plane on top of the substrate. The adjacent side of the Spidron fractal slot is equidistant from the upper and lower sides and at a distance d from the left side of the substrate. A seven-iterated Spidron fractal patch with length h_2 and angle β is placed inside the Spidron fractal slot and is displaced by n_1 and n_2 from the adjacent side of the Spidron fractal slot along the x-axis and y-axis, respectively. A rectangular slit of length s_y and width s_w protrudes outward from the Spidron fractal slot. This slit is positioned at a distance of x_1 from the vertex and rotated at an angle γ with respect to the hypotenuse

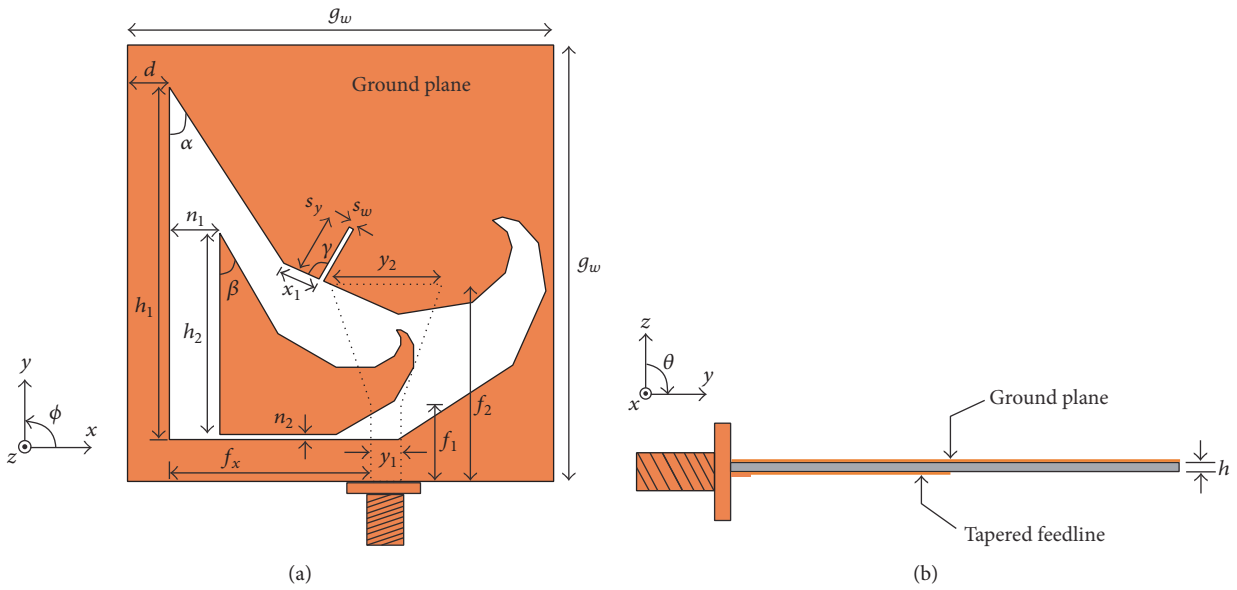

FIGURE 1: Geometry of the proposed antenna: (a) top view; (b) side view.

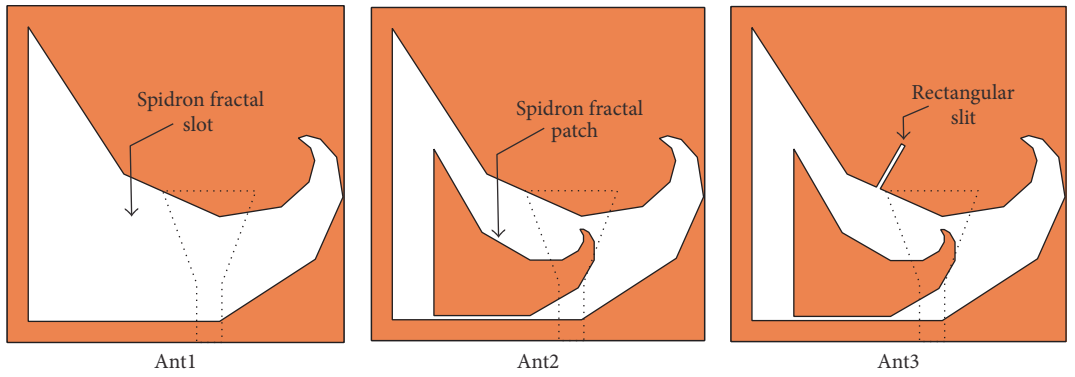

FIGURE 2: Geometries of Ant1, Ant2, and Ant3.

of the second right-angled triangle of the Spidron fractal slot. A tapered microstrip feedline of length f_2 and tapered-end width y_2 is attached to the bottom side of the substrate to excite the proposed antenna. The length and width of the feedline before tapering are f_1 and y_1, respectively. The feedline is displaced at a distance of f_x from the adjacent side of the Spidron fractal slot. The orientation of the surface current in the proposed antenna is such that it provides a left-handed circular polarization (LHCP) sense. The overall dimensions of the proposed antenna are $g_w \times g_w \times h$.

In order to validate the AR performance of the proposed antenna, three designs, a Spidron fractal slot (Ant1), a Spidron fractal slot with an embedded patch (Ant2), and a Spidron fractal slot with an added rectangular slit and an embedded patch (Ant3), are investigated. These designs are excited by tapered microstrip feedlines with identical dimensions. Figure 2 shows the geometry of these antennas; the simulated results of the reflection coefficient and AR are depicted in Figure 3. It was found that Ant1 achieves dual-band characteristics with regard to the reflection coefficient, as well as a narrow 3 dB AR bandwidth. The lower band has a −10 dB reflection bandwidth of 11.98% (3.61–4.07 GHz), while the AR bandwidth corresponds to 5.22% (3.92–4.13 GHz). However, the overlapping bandwidth, which satisfies both the reflection coefficient and the AR criteria, corresponds to 3.75% (3.92–4.07 GHz). For Ant2, which is designed with an embedded Spidron fractal patch based on the Ant1 design, a −10 dB reflection bandwidth of 50.53% (2.47–4.14 GHz) was noted, while dual-band characteristics were observed for AR as the level around 3.3 GHz is slightly higher than 3 dB. Consequently, with the addition of a rectangular slit to Ant2, termed Ant3, the AR level is lowered from 3 dB, resulting in a wide 3 dB AR bandwidth of 37.39% (2.74–4.00 GHz). In addition, a −10 dB reflection bandwidth of 49.62% (2.47–4.10 GHz) is achieved, nearly identical to that of Ant2.

To verify the sense of circular polarization, the simulated magnetic current distributions of a Spidron fractal slot with a time-varying phase at 3.5 GHz in $+z$-direction are depicted in Figure 4. It should be noted that the vectors (M_1, M_2, M_3, M_4) represent the major surface current distributions and that their sum is represented by M_{total}. For $t = 0$, as in Figure 4(a), the resultant vector M_{total} is directed

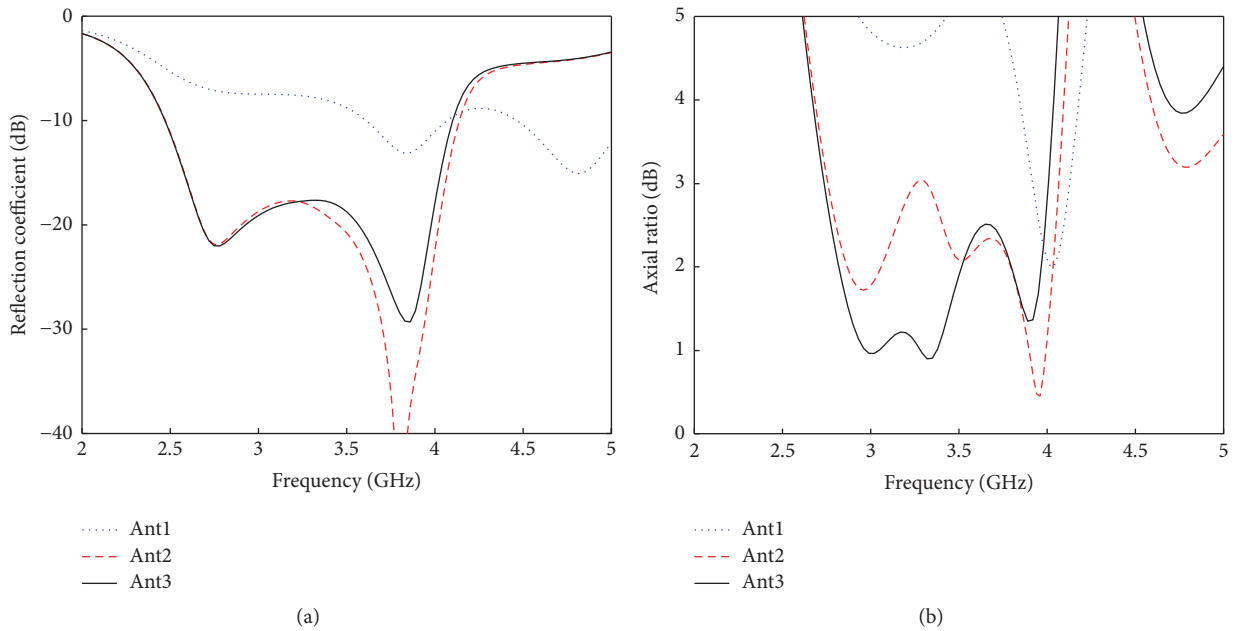

FIGURE 3: Comparison of Ant1, Ant2, and Ant3 in terms of (a) the reflection coefficient and (b) the axial ratio.

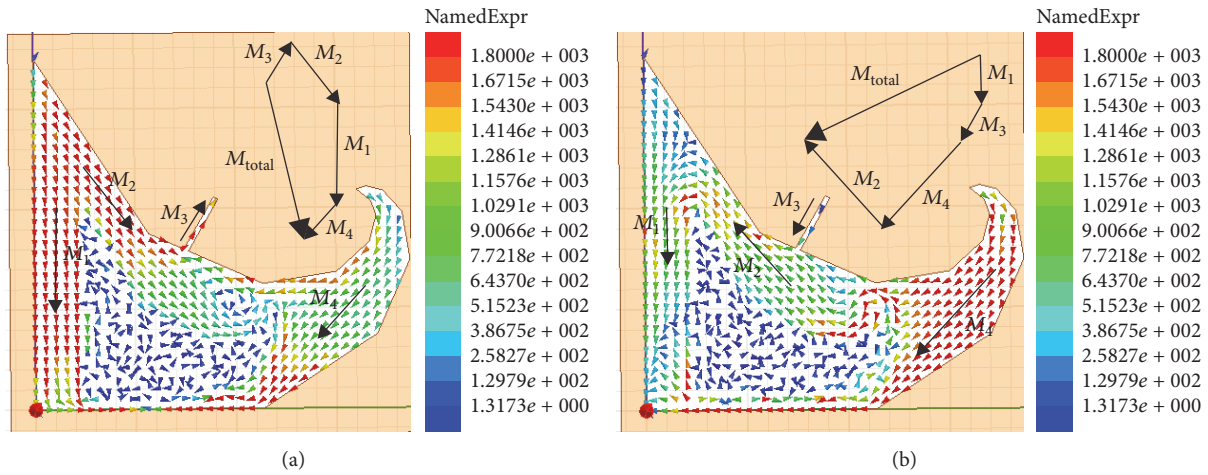

FIGURE 4: Simulated magnetic current distributions of a Spidron fractal slot with time period T at 3.5 GHz: (a) $t = 0$; (b) $t = T/4$.

towards lower right corner of the ground plane. When the phase changes to $t = T/4$, the resultant vector M_{total} rotates in a clockwise direction and becomes orthogonal to M_{total} in Figure 4(a). Therefore, the proposed antenna radiates LHCP waves.

3. Parametric Analysis

A parametric analysis is conducted in order to investigate the effects of varying the angle α of the Spidron fractal slot and the distance n_1 (between the Spidron fractal patch and the slot along the x-axis) on the reflection coefficient and the AR. These simulations are performed using the ANSYS High-Frequency Structure Simulator (HFSS) software. During this analysis, only one design parameter is allowed to change at a time.

The size of the Spidron fractal slot changes with the value of angle α; the effect of this variation on the reflection coefficient and AR is shown in Figure 5. In the figure, it is evident that an increase in angle α provides better impedance matching as the capacitance of the slot counterbalances the inductance of the tapered feedline. The 3 dB AR bandwidth is also very sensitive to the value of angle α and continues to widen as α is increased. For $\alpha = 30^\circ$ and $\alpha = 31.5^\circ$, dual-band CP characteristics are observed. The upper band, which lies around 4.5 GHz, does not satisfy the −10 dB reflection bandwidth criterion. When $\alpha = 33^\circ$, the CP bands of the Spidron fractal slot and patch lie close to each other; therefore, a wide 3 dB AR bandwidth is realized. A further increase in the value of angle α makes the proposed design unrealizable, as the size of the Spidron fractal slot does not fit within the given dimensions of the ground plane.

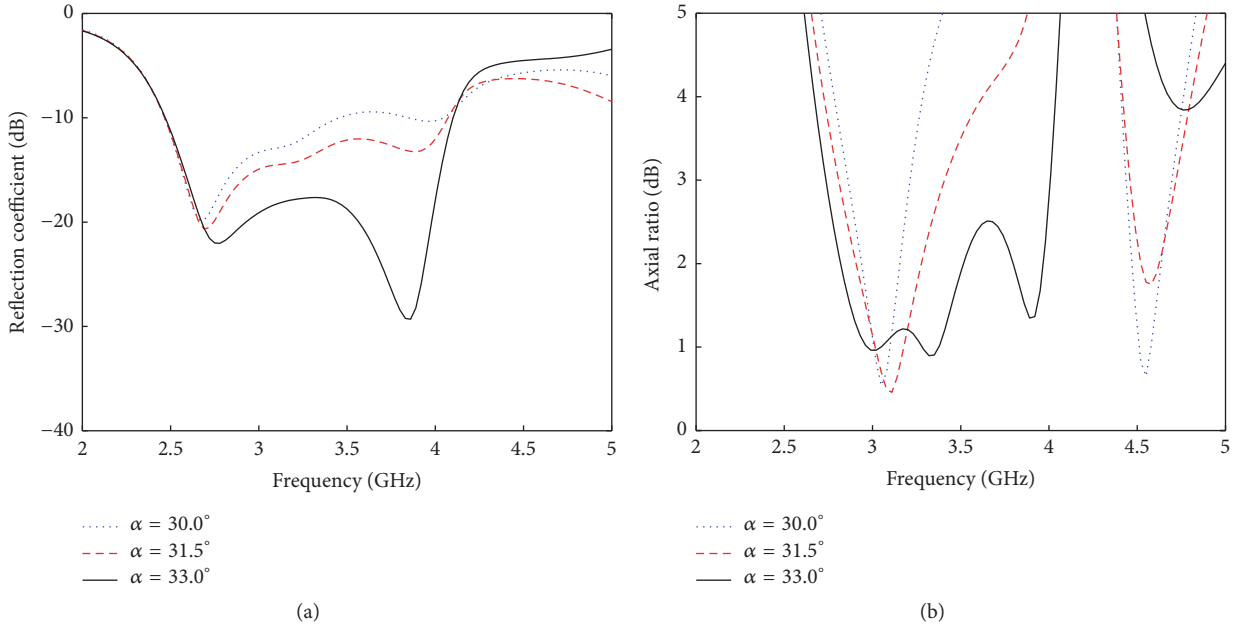

FIGURE 5: Effect of variation of angle α of the Spidron fractal slot on (a) the reflection coefficient and (b) the axial ratio.

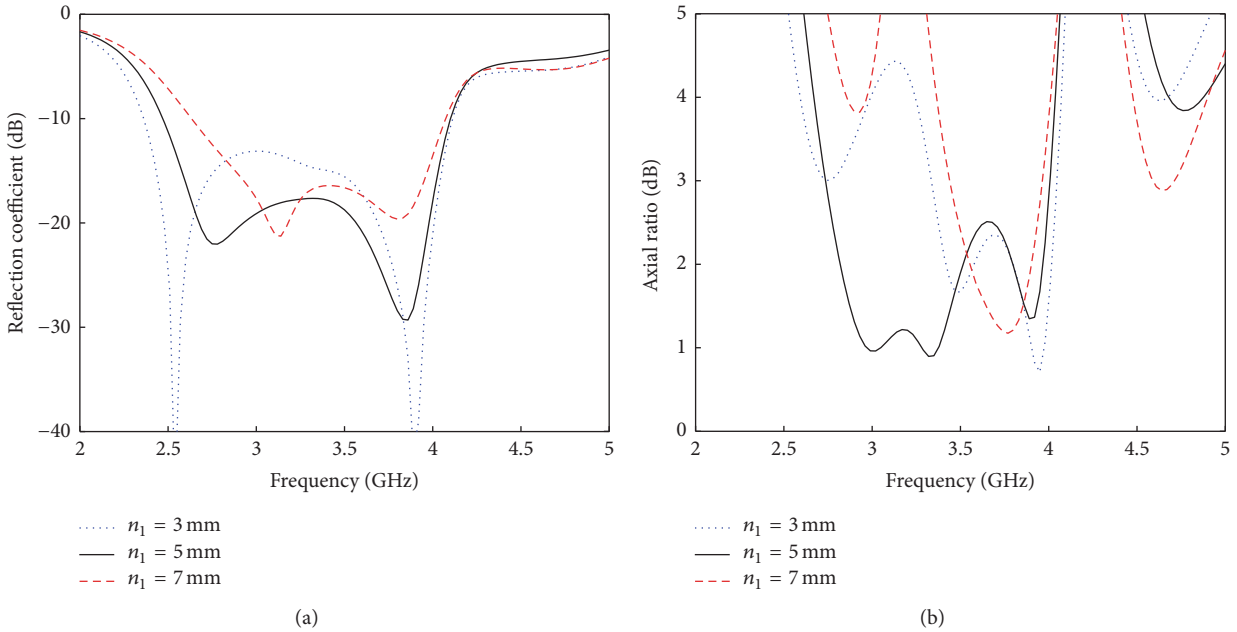

FIGURE 6: Effect of variation in distance n_1 on (a) the reflection coefficient and (b) the axial ratio.

The effect of variation of distance n_1 on the reflection coefficient and AR is depicted in Figure 6. It was observed that the −10 dB reflection bandwidth of the proposed design is determined by the variation of n_1 and that an increase in n_1 decreases the reflection bandwidth as the resonant bands of both structures move closer to one another. With this variation, the feeding position of the Spidron fractal patch is altered, which in turn modifies the surface current densities of the Spidron fractal slot and patch; hence the AR is subjected to variation. It was also noted that the upper CP band remains nearly identical, whereas the lower CP band is very sensitive to variations in n_1. While, for $n_1 = 3$ mm, the reflection bandwidth is the widest, the AR bandwidth is not as wide as compared to its width when $n_1 = 5$ mm. Therefore, on the basis of the AR performance, the chosen value is $n_1 = 5$ mm.

Based on the parameter analysis, the finally determined parameters of the proposed antenna are shown in Table 1.

4. Measurements and Discussion

After obtaining the optimum values of the design parameters from Table 1, a prototype of the proposed antenna was fabricated, as shown in Figure 7. The reflection coefficient of

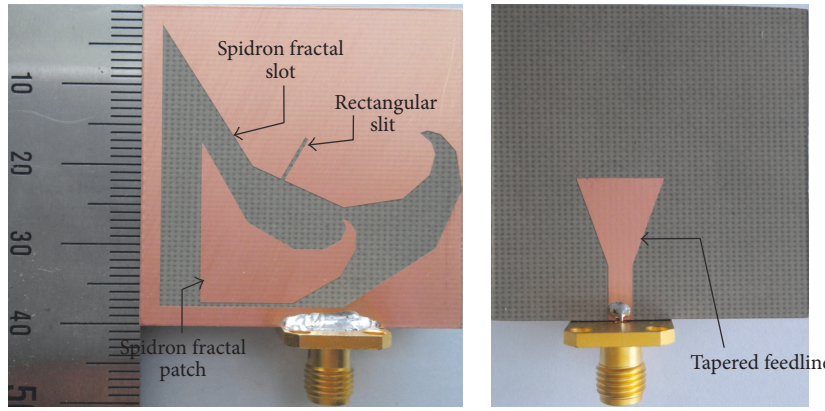

Figure 7: Photograph of the fabricated antenna: (a) top view; (b) bottom view.

Table 1: Geometric parameters of the proposed antenna.

Parameter	Value
h_1	35 mm
α	33°
h_2	20 mm
β	30°
n_1	5 mm
n_2	0.5 mm
h	1.52 mm
d	2.5 mm
g_w	40 mm
s_y	6 mm
s_w	0.5 mm
γ	96°
x_1	3.83 mm
f_2	18 mm
y_2	11.1 mm
f_x	20 mm
f_1	7 mm
y_1	3 mm

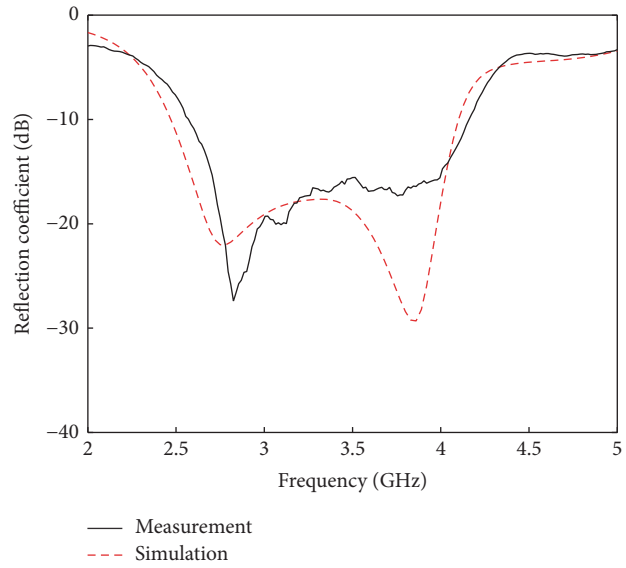

Figure 8: Measured and simulated reflection coefficients of the proposed antenna.

the fabricated antenna was measured using an Agilent 8510C network analyzer. Figure 8 depicts the results of a comparison of the measured and simulated reflection coefficients of the proposed design. The antenna attains measured and simulated −10 dB reflection bandwidths of 47.25% (2.57–4.16 GHz) and 49.62% (2.47–4.10 GHz), respectively. The discrepancy between the simulation and the measurement at the second resonant frequency band (3.8 GHz) can be attributed to the slight misalignment between the Spidron fractal slot on the top layer and the feedline on the bottom layer during the fabrication process. Figure 9 shows the measured and simulated ARs as well as the LHCP gains of the proposed antenna in the boresight direction ($\theta = 0^\circ$). The measured 3 dB AR bandwidth corresponds to 28.81% (3.09–4.13 GHz), while the simulated result is 37.39% (2.74–4.00 GHz). It is of practical importance to note that the total AR bandwidth lies within the reflection bandwidth; therefore, the overall AR bandwidth can be utilized for CP applications. These figures demonstrate that the measured results are in reasonably good agreement with the simulated results, apart from certain discrepancies which can be attributed to fabrication tolerance. The measured LHCP gain of proposed antenna varies from 2.12 dBic to 3.56 dBic within the AR bandwidth.

The measured and simulated radiation patterns of the proposed antenna on the xz ($\phi = 0^\circ$) and yz ($\phi = 90^\circ$) planes, for both the LHCP and right-handed circular polarization (RHCP) gains, at 3.6 GHz are shown in Figure 10. On both planes, the measured LHCP is stronger than the RHCP by more than 20 dB.

5. Conclusion

Based on the concept of an embedded design, a compact wideband CP Spidron fractal microstrip antenna was

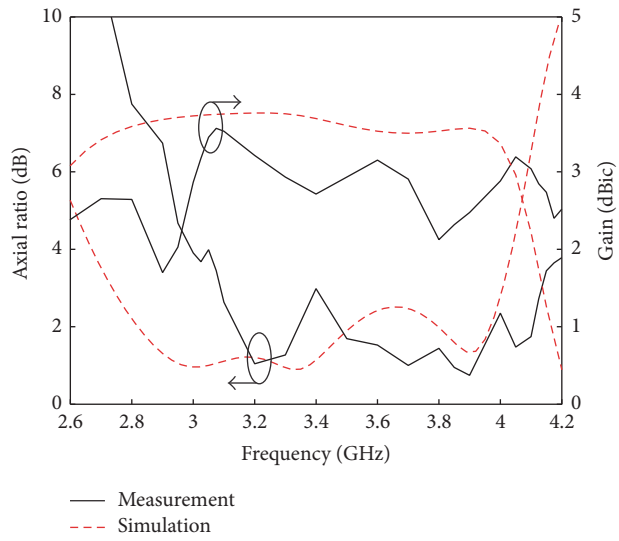

Figure 9: Measured and simulated axial ratios and LHCP gains of the proposed antenna.

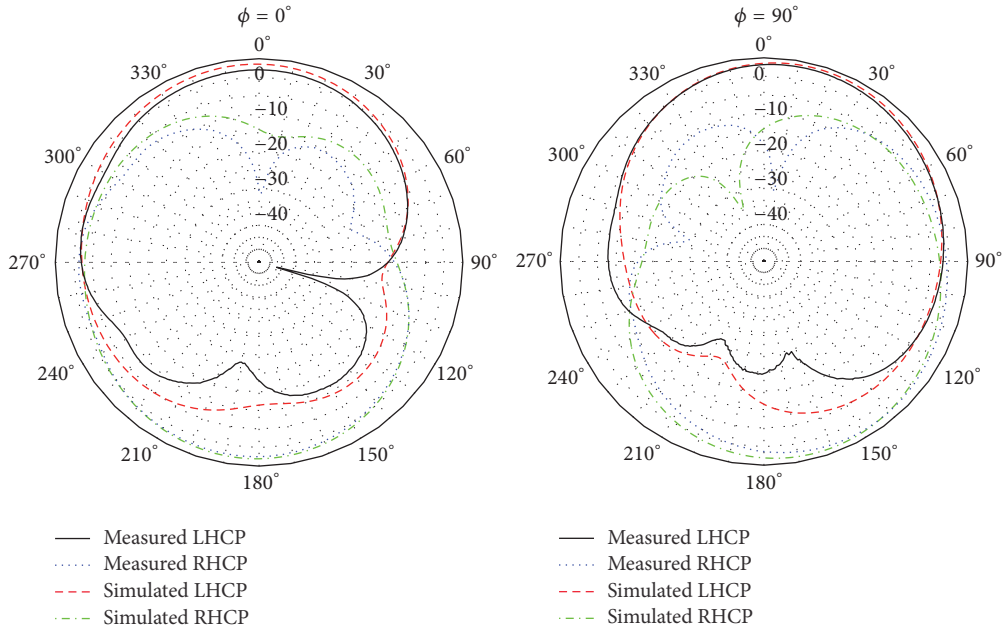

Figure 10: Measured and simulated radiation patterns of the proposed antenna at 3.6 GHz.

designed, fabricated, and tested. The experimental results have demonstrated that a wide 3 dB AR bandwidth of 28.81% is obtained in conjunction with a −10 dB reflection bandwidth of 47.25% when using the Spidron fractal slot and patch. In the boresight direction, the measured LHCP exceeds the RHCP by more than 20 dB. Therefore, the proposed design has the potential to be used in various CP applications owing to its structural simplicity.

Conflicts of Interest

The authors declare that they have no conflicts of interest.

Acknowledgments

This work was supported by the National Research Foundation of Korea (NRF) grant funded by the Korean government (MSIP) (2014R1A5A1011478).

References

[1] S. Tripathi, A. Mohan, and S. Yadav, "Hexagonal fractal ultra-wideband antenna using Koch geometry with bandwidth enhancement," *IET Microwaves, Antennas and Propagation*, vol. 8, no. 15, pp. 1445–1450, 2014.

[2] C. P. Baliarda, C. B. Borau, M. N. Rodero, and J. R. Robert, "An iterative model for fractal antennas: application to the Sierpinski gasket antenna," *IEEE Transactions on Antennas and Propagation*, vol. 48, no. 5, pp. 713–719, 2000.

[3] H. Oraizi and S. Hedayati, "Miniaturization of microstrip antennas by the novel application of the Giuseppe Peano fractal geometries," *IEEE Transactions on Antennas and Propagation*, vol. 60, no. 8, pp. 3559–3567, 2012.

[4] P. N. Rao and N. V. S. N. Sarma, "Minkowski fractal boundary single feed circularly polarized microstrip antenna," *Microwave and Optical Technology Letters*, vol. 50, no. 11, pp. 2820–2824, 2008.

[5] V. V. Reddy and N. V. S. N. Sarma, "Compact circularly polarized asymmetrical fractal boundary microstrip antenna for wireless applications," *IEEE Antennas and Wireless Propagation Letters*, vol. 13, pp. 118–121, 2014.

[6] H. A. Ghali and T. A. Moselhy, "Broad-band and circularly polarized space-filling-based slot antennas," *IEEE Transactions on Microwave Theory and Techniques*, vol. 53, no. 6, pp. 1946–1950, 2005.

[7] Nasimuddin, Z. N. Chen, and X. Qing, "Wideband circularly polarized slot antenna," in *Proceedings of the 42nd European Microwave Conference (EuMC '12)*, pp. 830–833, Amsterdam, The Netherlands, 2012.

[8] Nasimuddin, Z. N. Chen, and X. Qing, "Symmetric-aperture antenna for broadband circular polarization," *IEEE Transactions on Antennas and Propagation*, vol. 59, no. 10, pp. 3932–3936, 2011.

[9] S. J. Jeong, K. C. Hwang, and D.-I. Hwang, "Compact circularly polarized antenna with a capacitive feed for GPS/GLONASS applications," *ETRI Journal*, vol. 34, no. 5, pp. 767–770, 2012.

[10] K. C. Hwang, "Broadband circularly-polarised Spidron fractal slot antenna," *Electronics Letters*, vol. 45, no. 1, pp. 3–4, 2009.